

Multiplexed Protease Activity Assay for Low-Volume Clinical Samples Using Droplet-Based Microfluidics and Its Application to Endometriosis

Chia-Hung Chen,^{†,‡,§,#} Miles A. Miller,^{§,||,#} Aniruddh Sarkar,[†] Michael T. Beste,^{§,||} Keith B. Isaacson,^{||,⊥} Douglas A. Lauffenburger,^{§,||} Linda G. Griffith,^{§,||} and Jongyoon Han^{*,†,§}

[†]Department of Electrical Engineering and Computer Science, [§]Department of Biological Engineering, and ^{||}Center for Gynecopathology Research, Massachusetts Institute of Technology, Cambridge, Massachusetts 02139, United States

[‡]Department of Bioengineering, National University of Singapore, Singapore 117575

[⊥]Newton-Wellesley Hospital, Harvard Medical School, Newton, Massachusetts 02462, United States

Supporting Information

ABSTRACT: As principal degrading enzymes of the extracellular matrix, metalloproteinases (MPs) contribute to various pathologies and represent a family of promising drug targets and biomarker candidates. However, multiple proteases and endogenous inhibitors interact to govern MP activity, often leading to highly context-dependent protease function that unfortunately has impeded associated clinical utility. We present a method for rapidly assessing the activity of multiple specific proteases in small volumes (<20 μL) of complex biological fluids such as clinical samples that are available only in very limited amounts. It uses a droplet-based microfluidic platform that injects the sample into thousands of picoliter-scale droplets from a barcoded droplet library (DL) containing mixtures of unique, moderately selective FRET-based protease substrates and specific inhibitors and monitors hundreds of the reactions thus initiated simultaneously by tracking these droplets. Specific protease activities in the sample are then inferred from the reaction rates using a deconvolution technique, proteolytic activity matrix analysis (PrAMA). Using a nine-member DL with three inhibitors and four FRET substrates, we applied the method to the peritoneal fluid of subjects with and without the invasive disease endometriosis. The results showed clear and physiologically relevant differences with disease, in particular, decreased MMP-2 and ADAM-9 activities.

Extracellular proteases participate in myriad physiological and disease processes, most prominently by degrading extracellular matrix components. In particular, matrix metalloproteinases (MMPs) and a disintegrin and metalloproteinases (ADAMs) have been investigated as potential drug targets and diagnostic biomarkers. Metalloproteinase (MP) activities are regulated through a tight network of multiple proteolytic enzymes and inhibitors [especially tissue inhibitors of MPs (TIMPs)], frequently resulting in highly context-dependent behavior that has hampered their usefulness in the clinic. Existing approaches such as zymography,^{1a} activity-based ELISAs,^{1b} peptide microarrays,^{1c} and activity-based probes^{1d} have been limited by tradeoffs including throughput, simultaneous

measurement of multiple activities (multiplexing), cost, and direct kinetic measurement. Alternatively, fluorescence resonance energy transfer (FRET)-based polypeptides have been used in recently developed techniques^{1c,2} such as proteolytic activity matrix analysis (PrAMA) to ascertain multiple specific protease activities simultaneously.² The PrAMA technique interprets reaction rates from panels of moderately selective fluorogenic substrates combined with specific protease inhibitors to infer a profile of protease activities from relatively unprocessed physiological samples. Unfortunately, this approach involves performing separate parallel biochemical reactions and consequently carries large liquid-handling and material requirements, presenting a challenge in clinical applications with limited sample quantities.

Here we report the development and use of an integrated droplet-based microfluidics platform for initiating and simultaneously observing hundreds of protease enzyme activity reactions for hours (up to ~ 800 individual droplets under nine different sets of reaction conditions) using limited quantities (<20 μL) of biological/clinical samples and then deconvolving the observed reaction rates using PrAMA. Compartmentalizing the chemical reagents in picoliter-scale aqueous droplets allows for a potential 10^6 -fold reduction in reagent consumption compared with standard methods and facilitates the rapid monitoring of thousands of droplets, each of which may contain unique experimental conditions.³ Droplet-based technology has recently been applied to a variety of biological applications,⁴ and picoinjectors have recently been developed to perform multistep experiments efficiently for large-scale multiplexing.⁵ Integration of these capabilities with PrAMA confers particular synergy: the droplet microfluidics create large-scale parallel measurements of multiple protease activity reactions, while PrAMA efficiently interprets the high-dimensional kinetic data to infer multiple specific proteolytic activities.

We applied this method to study the invasive disease endometriosis, which is generally defined by the presence of endometrial-like tissue residing outside the uterus and is strongly associated with pain and infertility. MPs have been implicated as

Received: August 8, 2012

Published: November 18, 2012

important enzymes in endometriosis,⁶ but their activities in the context of dysregulated endogenous inhibitors remain less clear.^{6,7} Using the droplet-based multiplexed activity assay, we were able to analyze minimal amounts of clinically obtained peritoneal fluid (PF) from patients with and without endometriosis, and we found distinct patterns of protease activity for the disease and control samples. In particular, we discovered that MMP-2 and ADAM-9 enzymatic activity decreased with disease and concluded that MMP and TIMP concentrations alone failed to describe accurately the altered proteolytic turnover of specific enzymes. The microfluidic assay's multiplexing capability not only improved the discrimination between control and disease samples but also supported the inference of multiple, specific protease activities that would have been ambiguous or sample-limited using traditional approaches.

The complete method is schematized in Figure 1a, and device design, fabrication, and operation details are given in

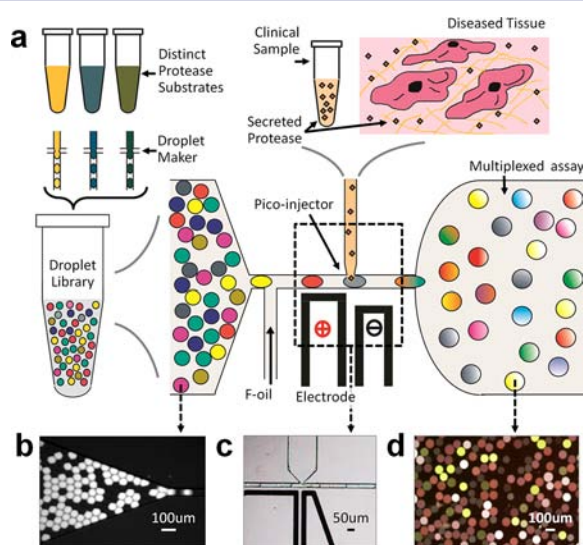


Figure 1. The microfluidic device. (a) Various protease activity substrates, and in some cases inhibitors, are encapsulated into the droplets, distinguished by optical dye labeling. The droplet library (b) flows into a picoinjector device (c) with high volume fraction order, where the droplets are merged with the biological sample. (d) Automated image processing is used to track the protease activity reaction in each droplet over time in an observation chamber.

Supplementary-1 in the Supporting Information (SI). We first prepared protease substrate libraries consisting of 50 μm diameter, monodisperse water-in-oil emulsions using droplet generator chips. We formulated droplets to encapsulate unique biochemical assays comprising aqueous solutions of particular protease substrates and, in some cases, protease inhibitors. PrAMA describes strategies for optimal selection of panels of substrates and inhibitors to infer specific protease activities accurately. In brief, multiple unique FRET substrates with distinct enzyme selectivity profiles can be utilized in parallel to permit computational inference of specific enzyme activities. This inference can be additionally strengthened by comparison of reaction rates in the presence or absence of specific inhibitors. In this application, we identify specific droplet compositions by optically "barcoding" them using specific concentrations of one or more indicator dyes (Alexa-405 and Alexa-546).³ The barcoded droplets are stabilized using an oil-phase surfactant and then mixed in a single tube, where they remain stable for >1

week. The generated droplet library (DL) is allowed to flow into the device (Figure 1b), where individual droplets containing protease substrates are mixed 1:1 with a fixed volume of biological sample containing proteases using a picoinjector (Figure 1c and movie si_005 in the SI).⁵ After they are mixed with the sample, the droplets flow to an integrated incubation chamber (Figure 1d), where they are monitored via time-lapse fluorescence microscopy for >3 h (see movie si_003 and the corresponding movie si_004 showing only the FRET kinetics). Hundreds of droplet reactions can be simultaneously monitored for hours using automated droplet tracking software, enabling both multiplexed capacity and accurate inference of reaction rates across multiple replicate droplets.

To establish the accuracy of microfluidic PrAMA (MF-PrAMA), we conducted reactions using recombinant enzymes. Purified enzyme solutions were injected into a DL consisting of four unique protease substrates (Supplementary-2) that were barcoded with Alexa-405. Sample-injected droplets were fluorescently imaged for 1.5 h (Figure 2a). Droplet tracking

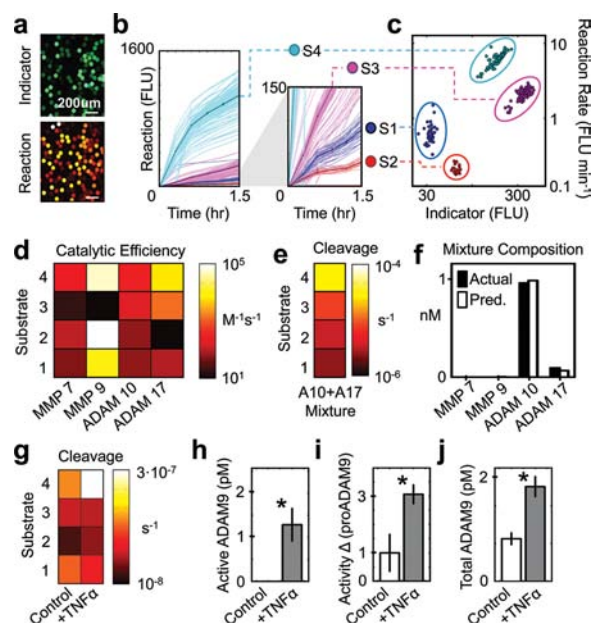


Figure 2. Application to purified enzymes and cell-based assays. (a) Droplet image of indicator dye and reaction product fluorescence. (b) Proteolysis of substrates S1–S4 was monitored by the fluorescence increase. Thick lines and error bars denote mean \pm SEM after (c) individual droplets (thin lines) were classified by their indicator dye and reaction rate. (d) Catalytic efficiencies were determined for samples with known concentrations of purified recombinant enzyme. (e) Observed cleavage rates for a mixture of recombinant ADAM-10 and ADAM-17. (f) PrAMA inferred the enzyme mixture from (e), using parameters from (d). (g) Substrate cleavage measured from 12Z-conditioned media. (h) ADAM-9 PrAMA results corresponding to (g). (i) Difference in S4 cleavages measured with and without proADAM-9. (j) ELISA results corresponding to (g–i) (*, $p < 0.05$).

software (Supplementary-3) was used to interpret the time-course images, and reaction rates were inferred from the increase in fluorescence resulting from substrate proteolysis (Figure 2b).² We gated the four DL components by their unique groupings of indicator fluorescence and reaction rate (Figure 2c). Enzyme catalytic efficiencies inferred from these groupings (Figure 2d) were compared to values obtained using a standard plate-reader assay ($R^2 > 95\%$ between the two assay formats; Supplementary-

4A). We inferred the composition of unknown enzyme mixtures on the basis of their observed substrate cleavage patterns with >95% accuracy (Figure 2e,f and Supplementary-4B,C).

After using purified enzymes to validate the device, we applied it to the in vitro study of an immortalized cell line (12Z) established from a peritoneal endometriotic biopsy.⁸ To ascertain the proteolytic activity response of these cells to TNF- α (an implicated inflammatory cytokine⁸), we stimulated cells for 24 h, collected and clarified the supernatant, and analyzed the samples with the aforementioned four-component DL (Figure 2g). It has been shown that MMP-2, MMP-9, and ADAM-9 are all secreted by 12Zs.⁸ We used MF-PrAMA specifically to analyze the activities of MMP-2, MMP-9, ADAM-9, and ADAM-10 (a known substrate of ADAM-9⁹). Of these enzymes, MF-PrAMA detected a significant increase only in ADAM-9 activity with TNF- α treatment ($p < 0.01$, bootstrapping test;² Figure 2h). To validate this result, we conducted activity assays with and without the specific ADAM-9 inhibitor proADAM-9 (Figure 2i).⁹ The results, combined with ADAM-9 ELISA data (Figure 2j), confirmed the upregulation of active ADAM-9 secretion ($p < 0.05$). By comparing the PrAMA and ELISA results, we found roughly 50% of ADAM-9 to be active, compared with <10% of MMP-2. This discrepancy is consistent with the high observed concentrations of TIMP-2, which does not inhibit ADAM-9 but does inhibit MMP-2 (Supplementary-5).¹⁰

We then analyzed PF from patients with moderate/severe endometriosis ($n = 7$) and compared the results to those for a control population without the disease ($n = 6$) (Supplementary-6). MF-PrAMA inference of specific protease activities revealed significant differences between disease and control samples. PF lines the pelvic cavity and comprises a heterogeneous mixture of leukocytes, cell debris, thousands of soluble proteins, and likely over 100 proteases and protease inhibitors that interact with endometriotic lesions.¹¹ We analyzed clarified PF samples using a nine-component substrate library consisting of the same four substrates used previously along with a broad-spectrum MP inhibitor (BB94), pro-domain inhibitors (PDIs) for ADAM-9 and ADAM-10,^{9,12} and buffer controls for the PDIs. The nine types of droplets were distinguished by their ratios of two indicator dyes (Figure 3a). Overall, the observed reaction rates (Figure 3b) showed the strongest activity with substrate S4, which can be efficiently cleaved by both MMPs and ADAMs (Supplementary-7A,C). Addition of BB94 reduced the observed rates by 90% on average, thereby confirming S4 cleavage to be principally the result of MPs. For most of the PF samples, droplets containing PDIs for ADAM-9 and ADAM-10 exhibited significantly lower reaction rates than their buffer controls. Across all of the samples, the ADAM-9 and ADAM-10 inhibitors reduced the reaction rates by an average of 25% ($\sigma = 16\%$) and 80% ($\sigma = 3\%$), respectively (Supplementary-7D). For six of the 13 PF samples, the summed proADAM-9/proADAM-10 inhibition accounted for roughly all of the observed S4 cleavage. We conducted PrAMA to infer specific protease activities from the cleavage measurements (Supplementary-3) and found ADAM-10 to be the most active protease in general. Of the MMPs, the PrAMA results suggested the activity of MMP-2 to be the highest on average (Supplementary-7E–G).

Significant correlation among the observed droplet reaction rates compelled the use of multivariate statistical approaches for data interpretation. We used partial least-squares discriminant analysis (PLS-DA) to describe patient status as a statistical function of multiple input variables (initially defined as the

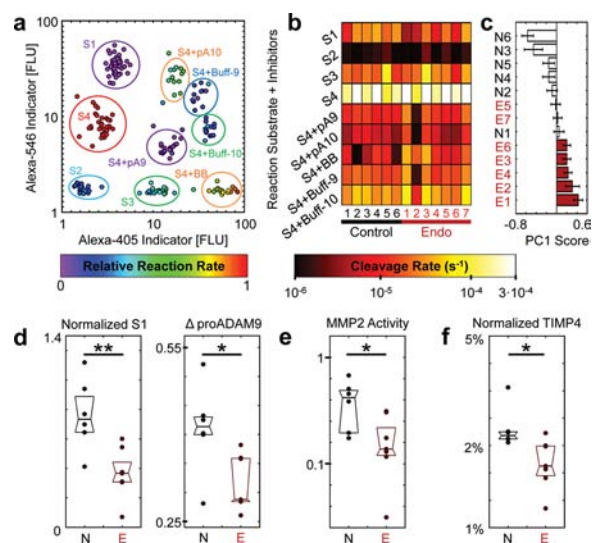


Figure 3. Clinical PF analysis. (a) Nine types of droplets were distinguished by two indicator dyes. (b) PF samples were analyzed from six nonendometriotic patients (“Control”) and seven patients with severe disease (“Endo”). The nine protease activity reactions measured for each clinical sample were defined by the substrate (S1–S4) and inhibitor (pA9 = proADAM-9, pA10 = proADAM-10, BB = BB94, Buff = buffer controls for the pro-domain inhibitors). (c) Plot of PLS-DA scores (\pm SEM) for classifying the disease status using the measurements shown in (b). (d) Box plots of the two most significant variables identified by PLS-DA, both of which significantly decreased in endometriotic patients. (e) The most significant PrAMA result corresponding to data in (b) as determined by PLS-DA. (f) TIMP-4 concentrations decreased significantly with disease, especially when normalized to the MMP-2 and TIMP-2 concentrations for each patient sample (**, $p < 0.01$; *, $p < 0.05$).

substrate cleavage measurements). Droplet data were first normalized by dividing the rates by their column averages (Figure 3b). PLS-DA iteratively selected the variables that most accurately predicted disease status, which in this case were from three reactions: S1 and S4 with proADAM-9 and S4 with the buffer control for proADAM-9 (Supplementary-8A). PLS-DA combined information from these three measurements to classify disease status with 95% accuracy [$p = 0.03$, permutation test (PT); Figure 3c].

The “normalized S1” rates statistically decreased with disease even when analyzed individually [$p = 0.042$, Mann–Whitney test, Bonferroni correction (M–W/B); Figure 3d]. On the basis of the PLS-DA modeling, we also investigated the difference in reaction rates with and without the proADAM-9 inhibitor (Δ proADAM-9) and found a decrease with disease ($p = 0.035$, M–W; Figure 3d). Since pro-ADAM-9 specifically inhibits ADAM-9, reduced Δ proADAM-9 can readily be interpreted as a decrease in ADAM-9 activity with disease. However, the interpretation of decreased S1 cleavage is less straightforward because S1 can be cleaved by multiple proteases (particularly MMPs, including MMP-2, rather than ADAMs). To address this issue, we utilized PrAMA inference to reveal significant differences in specific protease activities (rather than ambiguous differences in substrate cleavage) between disease and control samples. We used PLS-DA to identify the most significant PrAMA descriptors of disease status, which yielded an equally accurate four-component model (93% accuracy, $p = 0.04$, PT; Supplementary-8B,C) that ranked the MMP-2 activity as the most significant determinant (Supplementary-8B). We therefore

examined the relative MMP-2 activity individually and found it to decrease with disease ($p = 0.02$, M–W; Figure 3e). We performed ELISAs on the PF samples for MMP-2 and two of its endogenous inhibitors, TIMP-2, and TIMP-4, to determine whether changes in the MMP-2 activity reflected trends in the concentration (Supplementary-9). The results identified high levels of both MMP-2 and TIMP-2, but neither the absolute concentrations nor the MMP-2/TIMP-2 ratio significantly changed with disease. Rather, the TIMP-4 concentration significantly decreased with disease, particularly when divided by the average concentration of the three analytes for each patient sample ($p = 0.024$, M–W/B; Figure 3f). The nonintuitive concomitant decrease in the MMP-2 and ADAM-9 activities despite the reduced TIMP-4 inhibitor concentration suggests that endometriosis perturbs multiple, overlapping protease–inhibitor interactions in the peritoneal environment. This complexity highlights the challenges associated with inferring enzyme activities from concentration alone and emphasizes the need for multiplexed, direct activity measurements.

In summary, this work has created a platform for assessing multiple specific protease activity assays with minimal liquid handling and sample requirements by integrating several components, including a droplet generator,³ a picoinjector,⁵ and an analytical inference technique (PrAMA).² Accomplishing the same multiplexed measurements in a 96-well microtiter plate would consume roughly 100-fold more biological sample and reagent [20 μL of sample for the multiplexed microfluidic assay compared with a microtiter format requiring 80 μL of sample/well in triplicate with the nine reaction conditions (27 wells total)], which would be a prohibitively high amount, especially for clinical samples. It is further noteworthy that only a tiny fraction (~ 30 nL) of the 20 μL sample volume was actually utilized to generate droplets for multiplexed sensing because of the unoptimized world-to-chip interfacing. This leaves much room for efficiency improvement by increasing the degree of multiplexing or decreasing the sample volume needed. Integrated chip design that combines droplet generation with picoinjection, along with advanced droplet barcoding strategies, will be critical in advancing the multiplexing capabilities of the platform. Here we have presented proof-of-principle DLs utilizing three barcode colors and nanoparticle dyes (Supplementary-10), and previous work has shown the potential of using microparticles, quantum dots, and hydrogels for optical discrimination of potentially thousands of unique particles that have been found to be amenable to droplet encapsulation.¹³ While such large DLs may require additional optical setup, the future challenge for enhancing the multiplexing capabilities of our platform and its overall technological potential centers on the physical generation of the DL itself.¹⁴

Our results underscore the value of multiplexing with microfluidic platforms for clinical sample analysis. Cleavage of individual substrates cannot generally be understood to relate to specific proteases. Here, however, in the context of multiple reactions using inhibitors and distinct substrates, disease samples could be clearly distinguished from control samples, and specific enzyme activities could also be determined. Furthermore, results from the multiplexed assay provided a novel perspective into MMP/TIMP regulation in endometriosis (Supplementary-11). Previous studies have reported conflicting observations regarding MMP-2 levels in endometriosis patients, and direct evidence of protease activity in the context of multiple interacting TIMPs has proved inconsistent.^{6,7} Here, despite the absence of detectable changes in MMP-2 concentration, MF-PrAMA

revealed a significant decrease in MMP-2 activity with disease, which may help explain the frequent clinical observation of isolated endometriotic cysts that do not invade the surrounding tissue.⁷ Our microfluidic platform could be extended in various ways (Supplementary-12), and the device modularity ultimately makes it highly customizable for a variety of applications.

■ ASSOCIATED CONTENT

📄 Supporting Information

Detailed procedures and expanded discussions. This material is available free of charge via the Internet at <http://pubs.acs.org>.

■ AUTHOR INFORMATION

Corresponding Author

jyhan@mit.edu

Author Contributions

#C.-H.C. and M.A.M. contributed equally.

Notes

The authors declare no competing financial interest.

■ ACKNOWLEDGMENTS

We thank Dr. R. Sperling for help with surfactant synthesis and the NIH (P50-GM68762 and U54-CA112967), the DARPA Cipher Program, NUS (Startup Grant R-397-000-137-133), and the SMART Innovation Centre (ING12043-BIO) for support.

■ REFERENCES

- (1) (a) Kleiner, D. E.; Stetler-Stevenson, W. G. *Anal. Biochem.* **1994**, *218*, 325. (b) Lauer-Fields, J. L.; Nagase, H.; Fields, G. B. *J. Biomol. Technol.* **2004**, *15*, 305. (c) Gosalia, D. N.; Denney, W. S.; Salisbury, C. M.; Ellman, J. A.; Diamond, S. L. *Biotechnol. Bioeng.* **2006**, *94*, 1099. (d) Sieber, S. A.; Niessen, S.; Hoover, H. S.; Cravatt, B. F. *Nat. Chem. Biol.* **2006**, *2*, 274.
- (2) Miller, M. A.; Barkal, L.; Jeng, K.; Herrlich, A.; Moss, M.; Griffith, L. G.; Lauffenburger, D. A. *Integr. Biol.* **2011**, *3*, 422.
- (3) (a) Agresti, J. J.; Antipov, E.; Abate, A. R.; Ahn, K.; Rowat, A. C.; Baret, J. C.; Marquez, M.; Klibanov, A. M.; Griffiths, A. D.; Weitz, D. A. *Proc. Natl. Acad. Sci. U.S.A.* **2010**, *107*, 4004. (b) Brouzes, E.; Medkova, M.; Savenelli, N.; Marran, D.; Twardowski, M.; Hutchison, J. B.; Rothberg, J. M.; Link, D. R.; Perrimon, N.; Samuels, M. L. *Proc. Natl. Acad. Sci. U.S.A.* **2009**, *106*, 14195.
- (4) (a) Zheng, B.; Roach, L. S.; Ismagilov, R. F. *J. Am. Chem. Soc.* **2003**, *125*, 11170. (b) Miller, O. J.; et al. *Proc. Natl. Acad. Sci. U.S.A.* **2012**, *109*, 378. (c) Chen, C. H.; Sarkar, A.; Song, Y. A.; Miller, M. A.; Kim, S. J.; Griffith, L. G.; Lauffenburger, D. A.; Han, J. *J. Am. Chem. Soc.* **2011**, *133*, 10368.
- (5) Abate, A. R.; Hung, T.; Mary, P.; Agresti, J. J.; Weitz, D. A. *Proc. Natl. Acad. Sci. U.S.A.* **2010**, *107*, 19163.
- (6) Szamatowicz, J.; Laudanski, P.; Tomaszewska, I. *Hum. Reprod.* **2002**, *17*, 284.
- (7) Gilabert-Estellés, J.; et al. *Hum. Reprod.* **2003**, *18*, 1516.
- (8) (a) Grund, E. M.; Kagan, D.; Tran, C. A.; Zeitvogel, A.; Starzinski-Powitz, A.; Nataraja, S.; Palmer, S. S. *Mol. Pharmacol.* **2008**, *73*, 1394. (b) Banu, S. K.; Lee, J. H.; Starzinski-Powitz, A.; Arosh, J. A. *Fertil. Steril.* **2008**, *90*, 972.
- (9) Moss, M. L.; et al. *J. Biol. Chem.* **2011**, *286*, 40443.
- (10) Amour, A.; et al. *FEBS Lett.* **2002**, *524*, 154.
- (11) Amon, L. A.; et al. *PLoS One* **2010**, *5*, No. e11137.
- (12) Moss, M. L.; et al. *J. Biol. Chem.* **2007**, *282*, 35712.
- (13) (a) Pregibon, D. C.; Toner, M.; Doyle, P. S. *Science* **2007**, *315*, 1393. (b) Abate, A. R.; Chen, C. H.; Agresti, J. J.; Weitz, D. A. *Lab Chip* **2009**, *9*, 2628.
- (14) Guo, M. T.; Rotem, A.; Heyman, J. A.; Weitz, D. A. *Lab Chip* **2012**, *12*, 2146.